

Electronic Supplementary Information (ESI)

Implementation of iMiDEV, a new fully automated microfluidic platform for radiopharmaceutical production

Olga Ovdiihuk,^a Hemantha Mallapura,^b Florian Pineda,^c Virginie Hourtané,^c Bengt Långström^d, Christer Halldin^b
Sangram Nag^b, Fatiha Maskali,^a Gilles Karcher^{a,e} and Charlotte Collet^{*a,f}

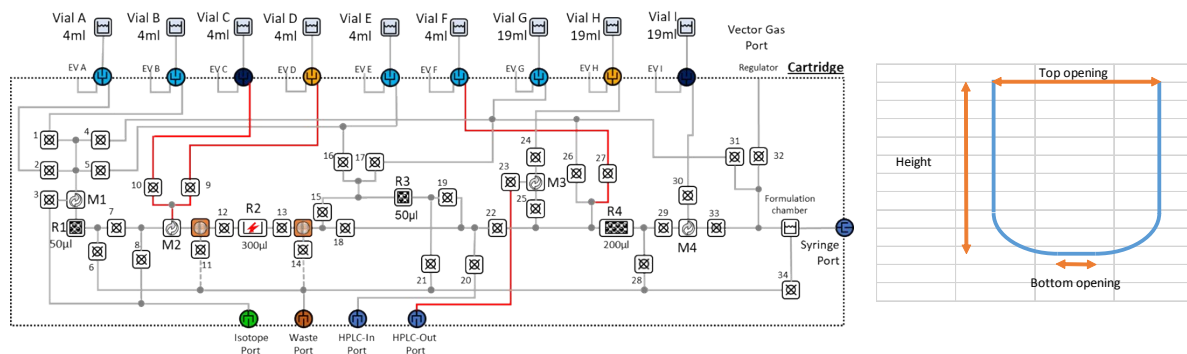
^{a.} *NancycloTEP, Molecular imaging platform, 54500 Vandoeuvre les Nancy, France*
^{b.} *Department of Clinical Neuroscience, Center for Psychiatry Research, Karolinska Institutet and Stockholm County Council, Stockholm 17176, Sweden*
^{c.} *PMB Alcen, Route des Michels CD56, 13790 Peynier, France*
^{d.} *Department of Chemistry, Uppsala University, Sweden*
^{e.} *CHRU-Nancy, France*
^{f.} *Université de Lorraine, INSERM U1254 IADI, F-54500 Vandoeuvre les Nancy, France*

Table of Contents

Table S1. Dimensions of channels, mixers and reactors	p 2
Figure S1. Location of holes for filling chambers with beads, pillars and pneumatic valves; top view of the cassette	
Figure S2. Cassette and vials clamping system	p 3
Figure S3. Schematic representation of the steps used for [¹⁸ F]NaF synthesis in R1 chamber	p 4
Table S2. Optimised sodium [¹⁸ F]fluoride synthesis data (n=16)	p 5
Figure S4. Graphical representation of [¹⁸ F]NaF Radiochemical Yield vs concentration of initial radioactivity of Fluoride-18	p 6
Figure S5. Graphical representation of [¹⁸ F]NaF Radiochemical Yield vs the volume of initial radioactivity of Fluoride-18	p 6
Figure S6. Schematic representation of the steps used for [¹⁸ F]NaF synthesis in R3 chamber	p 7
Figure S7. Trap-release radioactivity curve obtained after [¹⁸ F]NaF synthesis on R3 chamber	p 8
Figure S8. Schematic representation of the steps used for double [¹⁸ F]NaF synthesis	p 8-10
Figure S9. CLI of activity distribution for [¹⁸ F]NaF synthesis on R3: a) Cerenkov image after ¹⁸ F-trapping on R3 (136 MBq); b) white light image of the cassette; c) merged Cerenkov and white light images after ¹⁸ F-trapping step.	p. 10
Figure S10. CLI of residual activity distribution for [¹⁸ F]NaF synthesis on R1 (≤ 7 MBq, 3,7%): a) Cerenkov image after synthesis; b) white light image of the cassette; c) merged Cerenkov and white light images after completion of the synthesis.	p. 10
Figure S11. Gamma Ray spectre of [¹⁸ F]NaF	p 11
Figure S12. Representative analytical radio-HPLC profile of [¹⁸ F]NaF synthesized on R1	p 11

Table S1. Dimensions of channels, mixers and reactors

Dimensions (μm)	Big channels (grey)	Mixer channel (M1-M4)	Small channels (red)
Top opening	600	800	200
Bottom opening	140	320	10
Height	400	400	200



Dimensions (μm)	R1	R2	R3	R4
Width	5500	35900	5500	8000
Length	10700	12000	10700	26700
Depth	1000	1000	1000	1000
Volume (μL)	51	300	51	200

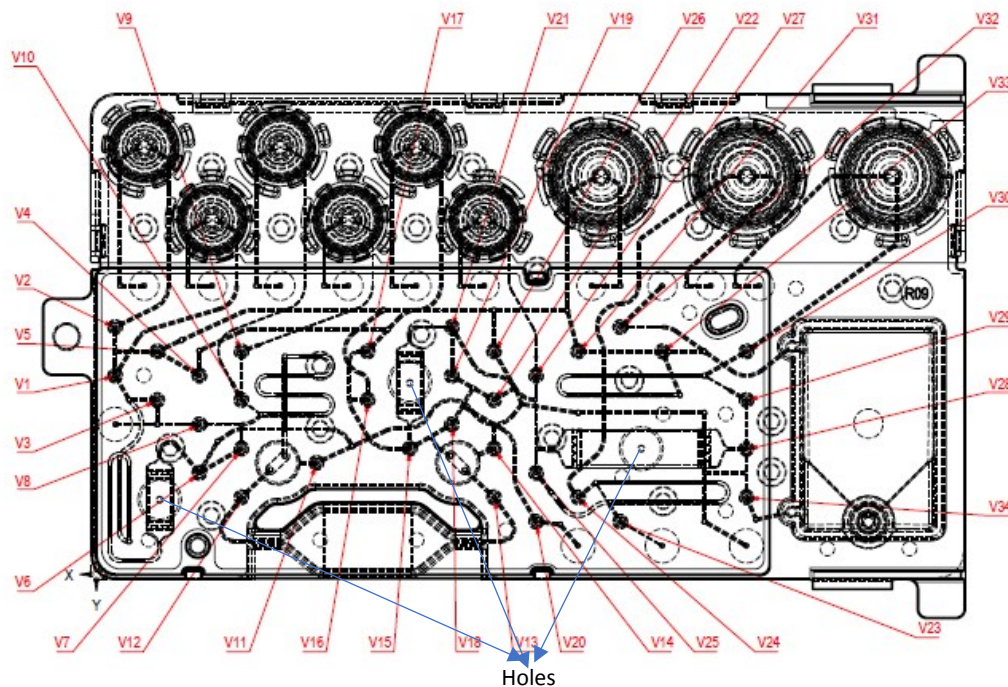
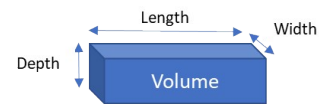
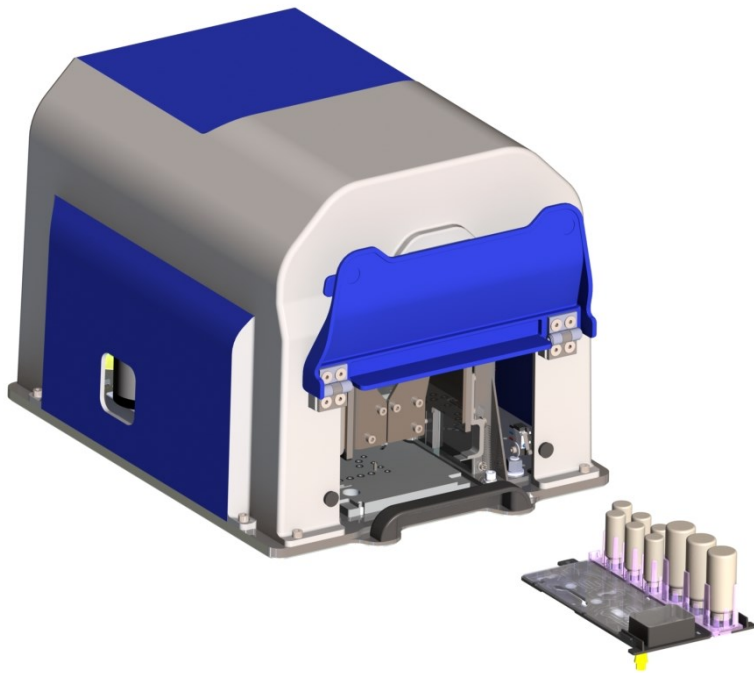
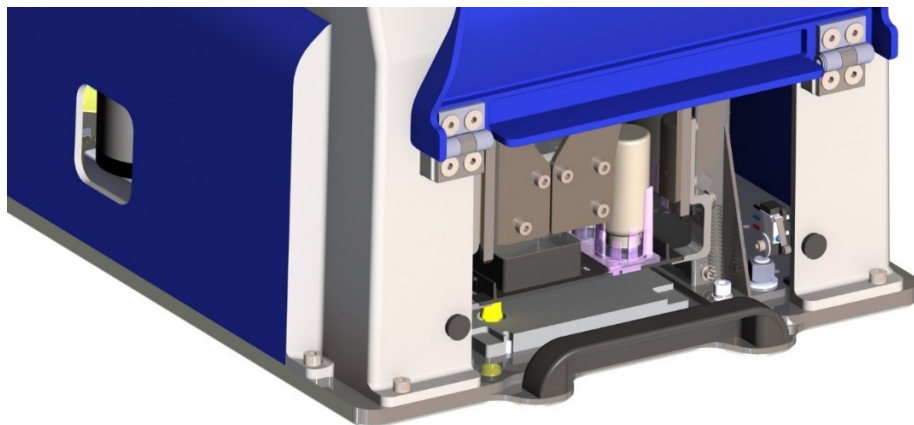


Figure S1. Location of holes for filling chambers with beads, pillars and pneumatic valves; top view of the cassette

a) Cassette presented



b) Cassette placed



c) Cassette clamped

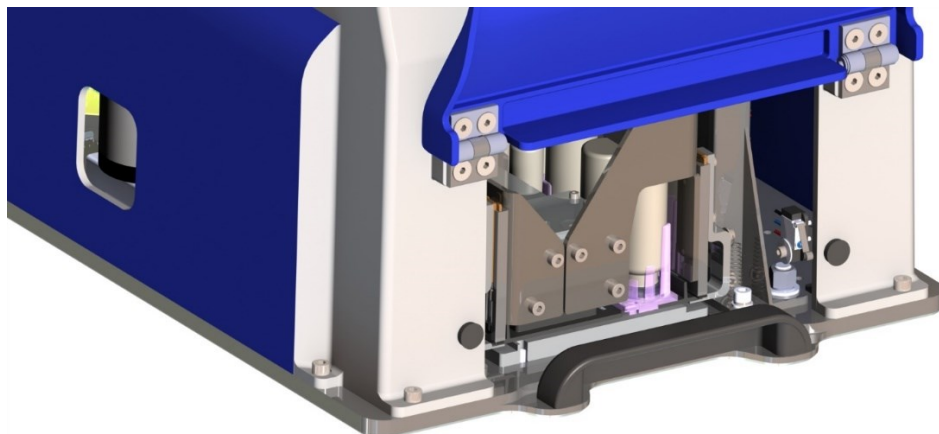


Figure S2. Cassette and vials clamping system; cassette external dimensions are 100x190x4 mm (l_xwxh, h=77 mm with vial holder and vials).

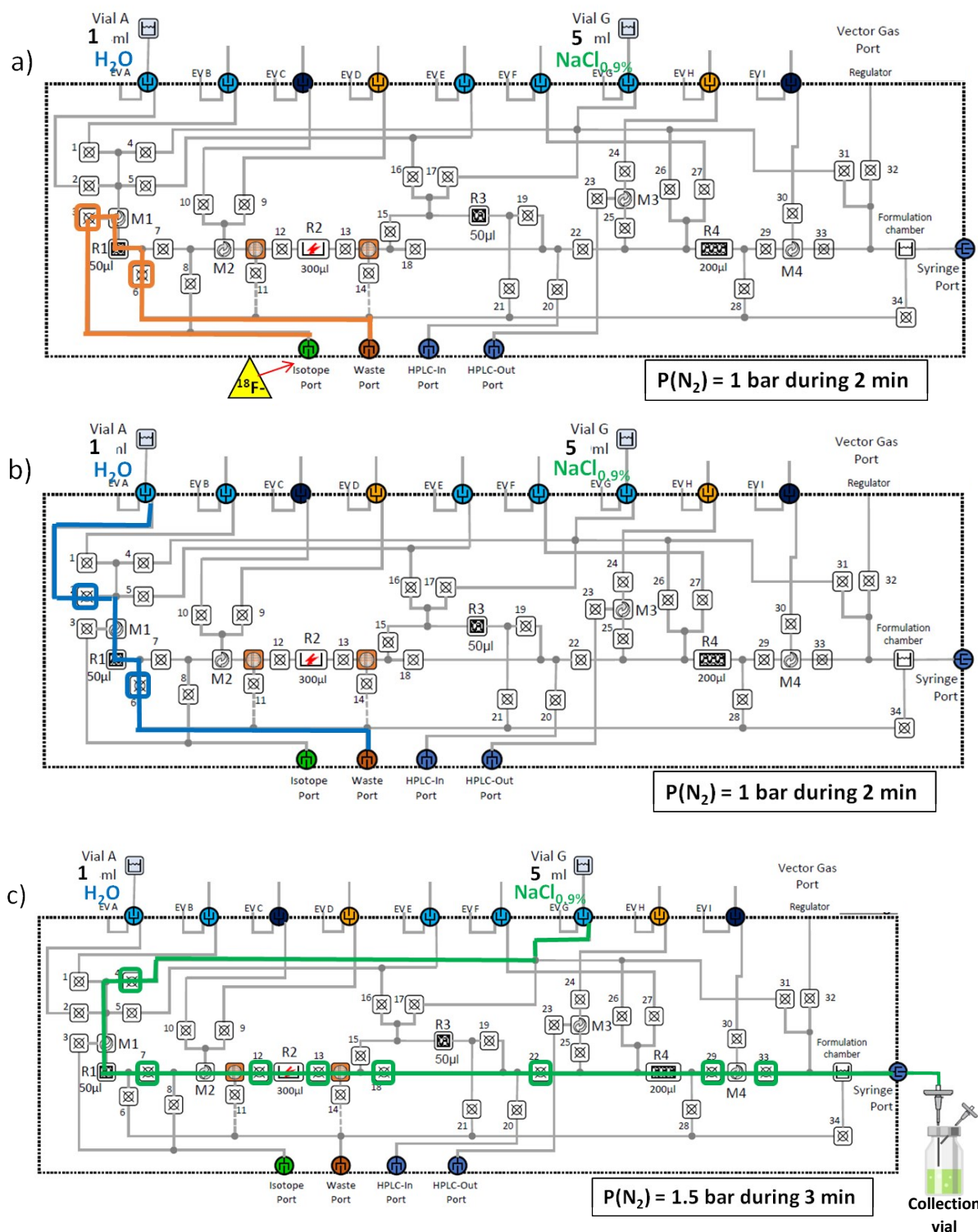


Figure S3. Schematic representation of the steps used for $[^{18}\text{F}]\text{NaF}$ synthesis in R1 chamber: a) activity reception ; b) washing; c) elution and delivery of $[^{18}\text{F}]\text{NaF}$.

Table S2. Optimised sodium [¹⁸F]fluoride synthesis data (n=16)

Entry	Chamber ^a	Target type	Initial activity of Fluoride-18 ^b , MBq	Volume of Fluoride-18, μL	C (Fluoride-18), MBq/mL	[¹⁸ F]NaF (dc to the SOS), MBq	RCY(dc), %
1	R1	Niobium	213	800	266	173	82
2	R1	Niobium	215	1600	134	177	85
3	R1	Niobium	209	850	246	161	78
4	R1	Niobium	203	450	451	127	65
5	R1	Niobium	198	500	396	132	69
6	R1	Silver	186	1500	124	161	87
7	R1	Niobium	214	600	357	158	75
8	R1	Silver	1609	1500	1073	1378	86
9	R1	Niobium	281	2500	112	247	91
10	R1	Niobium	228	800	285	179	79
11	R1	Niobium	225	700	321	167	76
12	R3	Niobium	122	2500	49	106	88
13	R3	Niobium	227	2000	114	200	88
14	R3	Niobium	306	2150	142	259	88
15	R3	Silver	574	2100	273	474	86
16	R3	Silver	713	3300	216	598	84

^a QMA-Cl beads reactivated with 0.9% NaCl; ^b at the SOS -start of synthesis; dc – decay corrected; RCY(dc)= $\frac{[[^{18}\text{F}]\text{NaF (dc to the SOS)}]}{([[\text{Initial activity of F-18}] - [\text{Activity of Fluoride-18 in the source vial}]] - [\text{Activity of Fluoride-18 in the vial}])}$

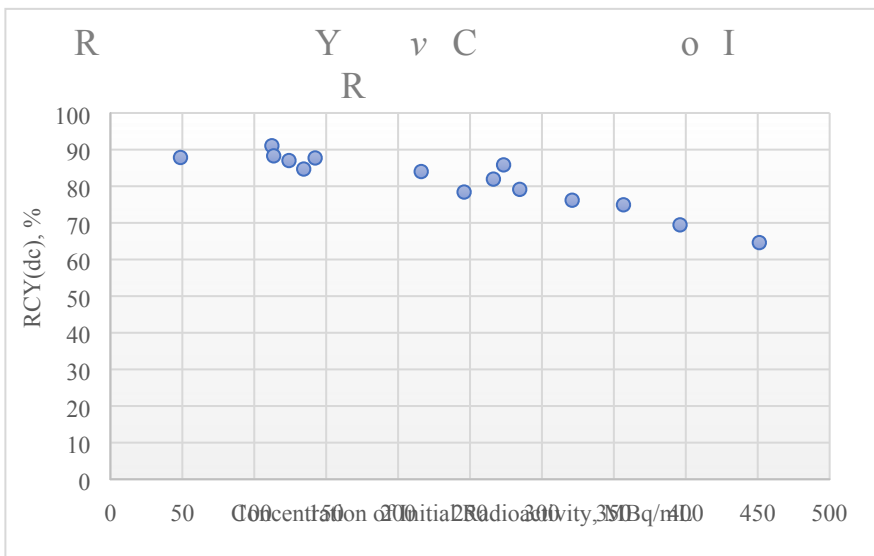
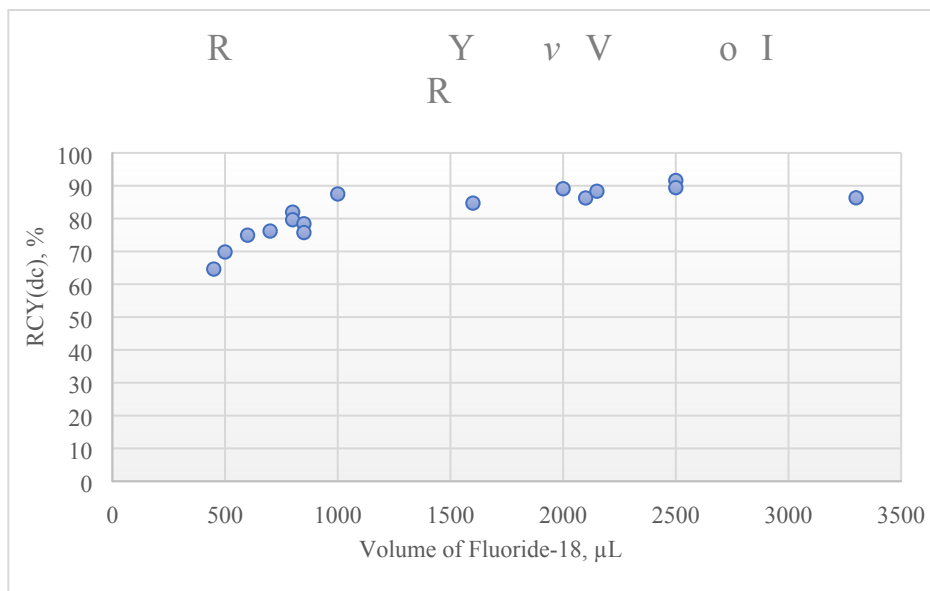


Figure S4. Graphical representation of [¹⁸F]NaF Radiochemical Yield vs concentration of initial radioactivity of Fluoride-18



Volume of Fluoride-18, μL	[¹⁸ F]NaF RCY(dc), %
450	65
500	69
600	75
700	76
800	82
800	79
850	78
1500	87
1500	86
1600	85
2000	88
2100	86
2150	88
2500	88
2500	91
3300	84

Figure S5. Graphical representation of [¹⁸F]NaF Radiochemical Yield vs the volume of initial radioactivity of Fluoride-18

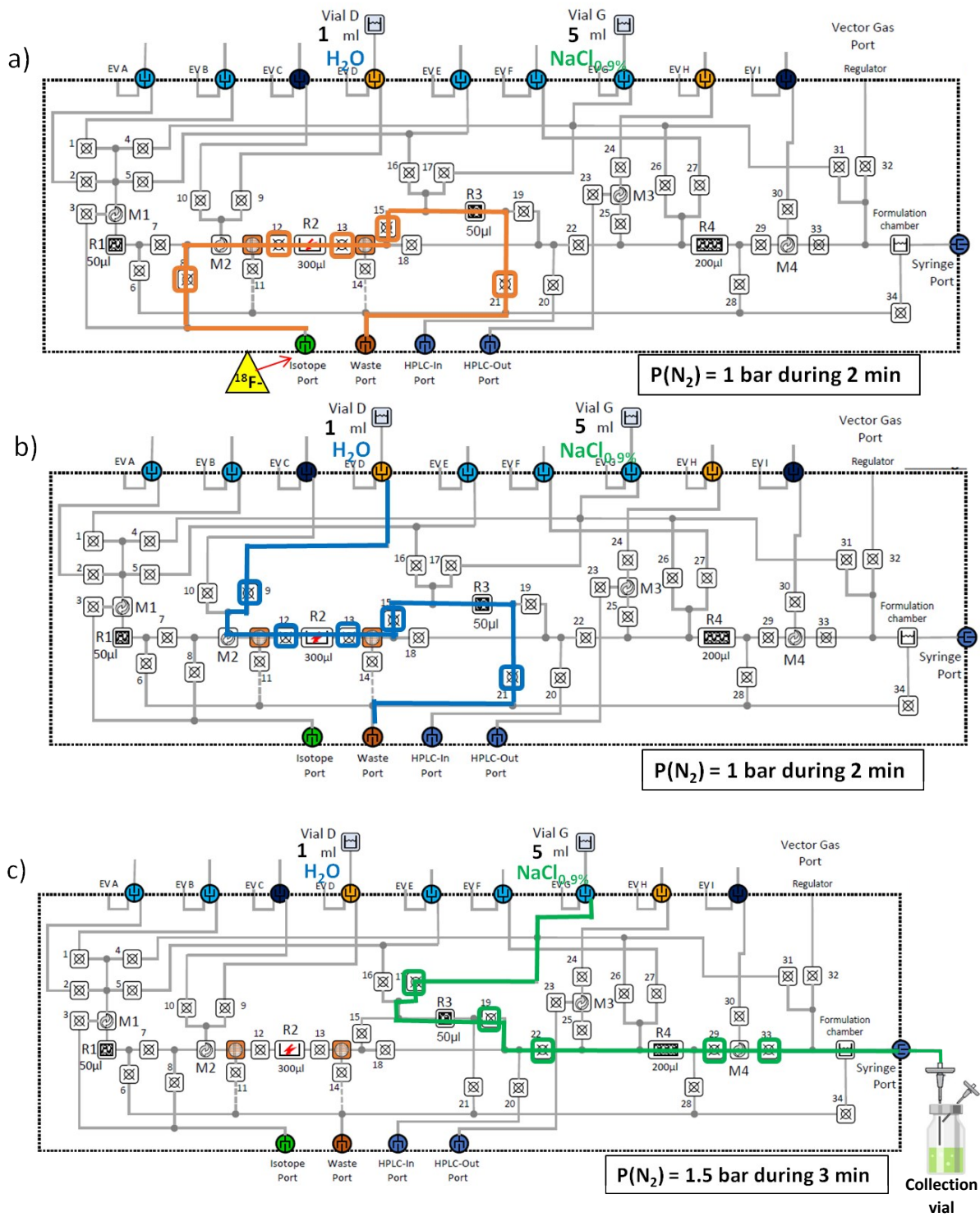


Figure S6. Schematic representation of the steps used for [¹⁸F]NaF synthesis in R3 chamber

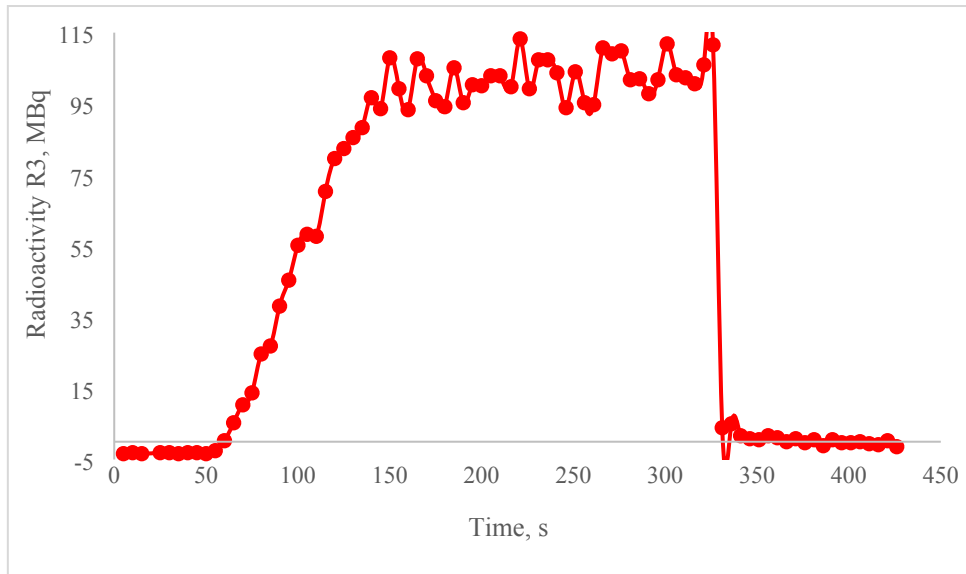
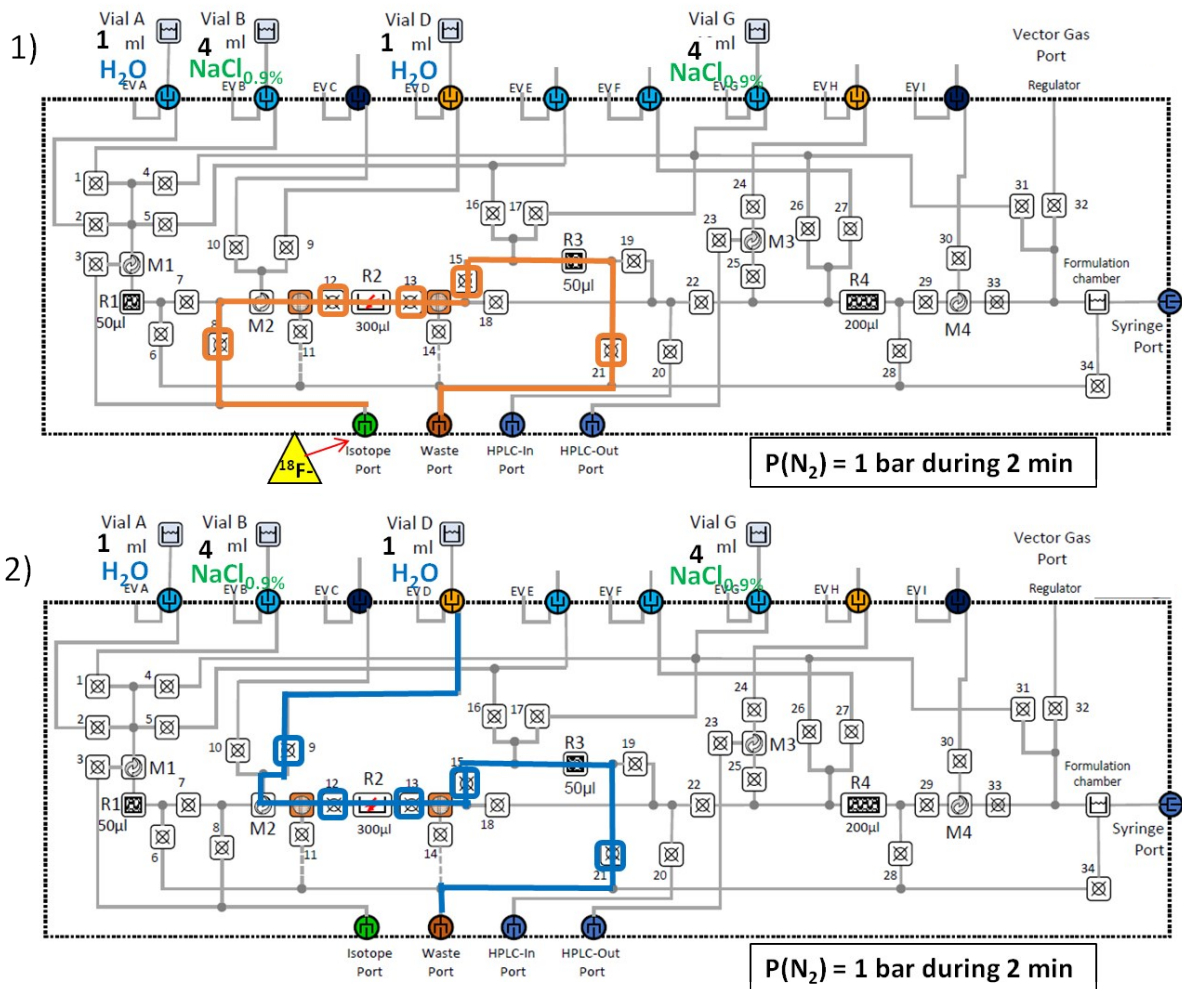
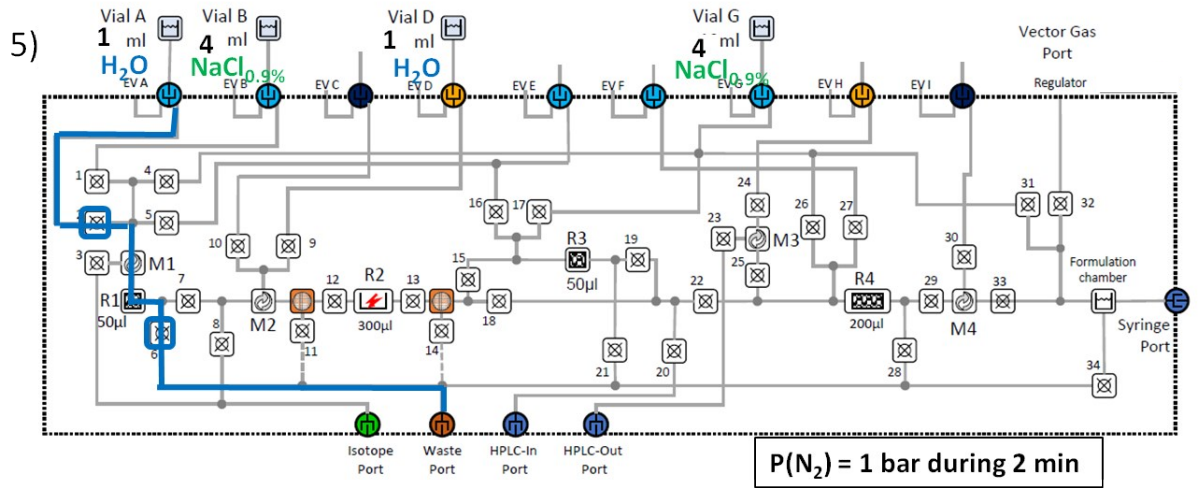
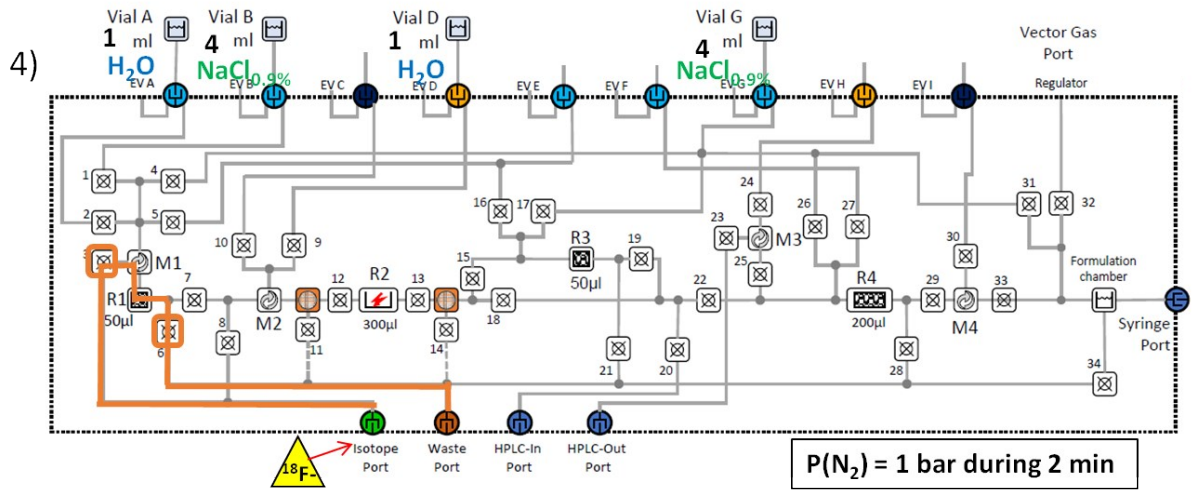
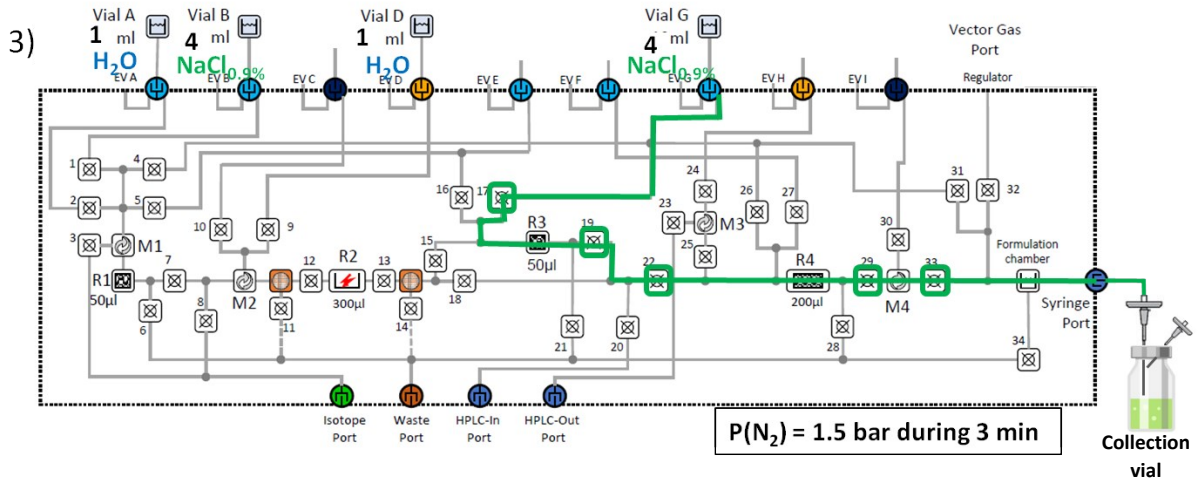


Figure S7. Trap-release radioactivity curve obtained after $[^{18}\text{F}]\text{NaF}$ synthesis on R3 chamber; 105 MBq of activity was concentrated from 2 mL of irradiated target $[^{18}\text{F}]\text{fluoride}$ solution





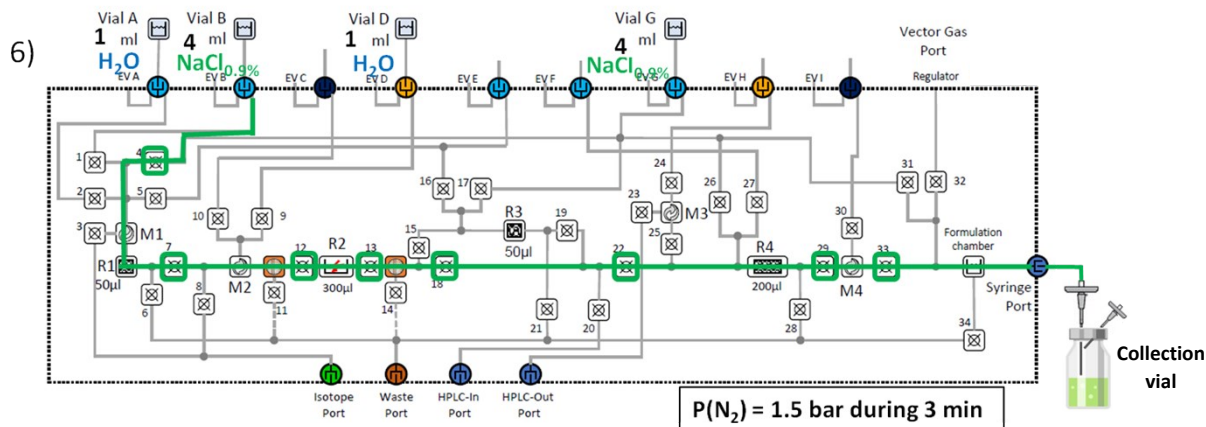


Figure S8. Schematic representation of the steps used for double $[^{18}\text{F}]\text{NaF}$ synthesis on R3 followed by R1: 1) activity reception: the fluoride-18 solution is transferred into injection port of the cassette and trapped on the QMA-Cl in chamber R3; 2) washing of R3 with sterile distilled water; 3) elution of fluoride-18 from R3 with 0,9% NaCl and a final $[^{18}\text{F}]\text{NaF}$ delivery from the formulation chamber to the collection vial; 4) activity reception: the fluoride-18 solution is transferred into injection port of the cassette and trapped on the QMA-Cl in chamber R1; 5) washing of R1 with sterile distilled water; 6) elution of fluoride-18 from R1 with 0,9% NaCl and a final $[^{18}\text{F}]\text{NaF}$ delivery from the formulation chamber to the collection vial.

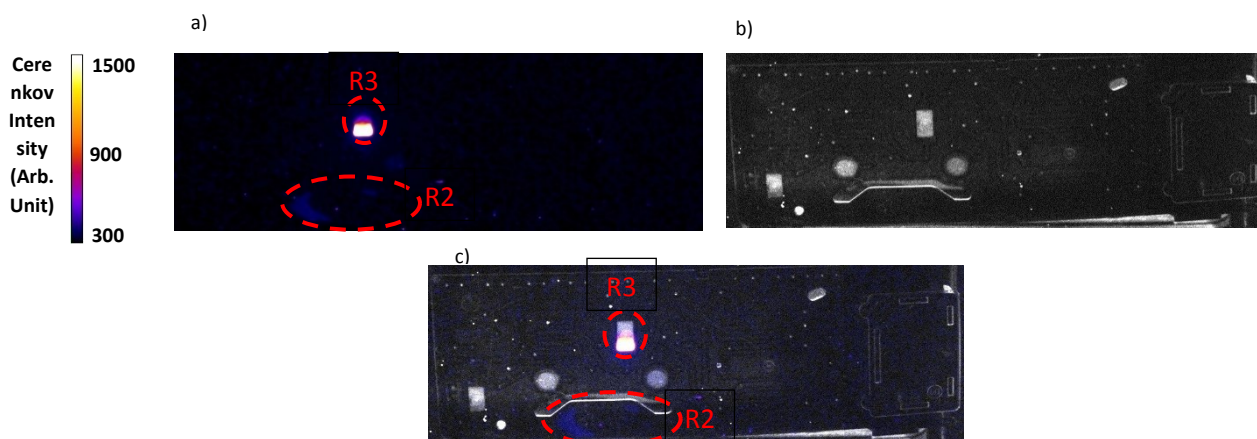


Figure S9. CLI of activity distribution for $[^{18}\text{F}]\text{NaF}$ synthesis on R3: a) Cerenkov image after ^{18}F -trapping on R3 (136 MBq) showing residual activity in R2; b) white light image of the top of the cassette; c) merged Cerenkov and white light images after ^{18}F -trapping step.

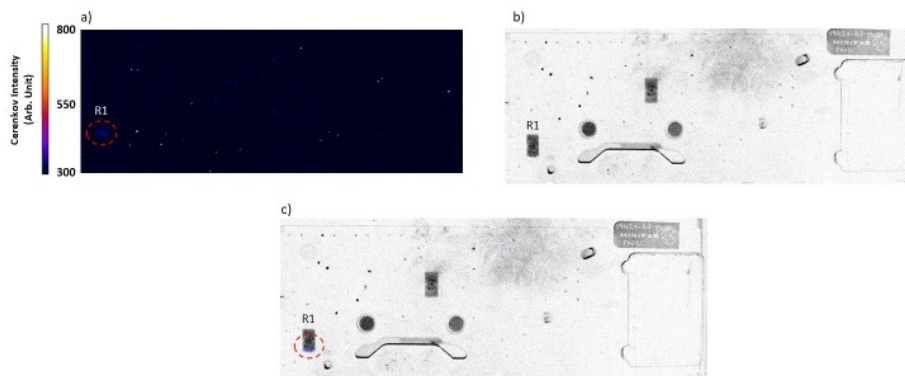


Figure S10. CLI of residual activity distribution for $[^{18}\text{F}]\text{NaF}$ synthesis on R1 (≤ 7 MBq, 3,7%): a) Cerenkov image after synthesis; b) white light image of the top of the cassette; c) merged Cerenkov and white light images after completion of the synthesis.

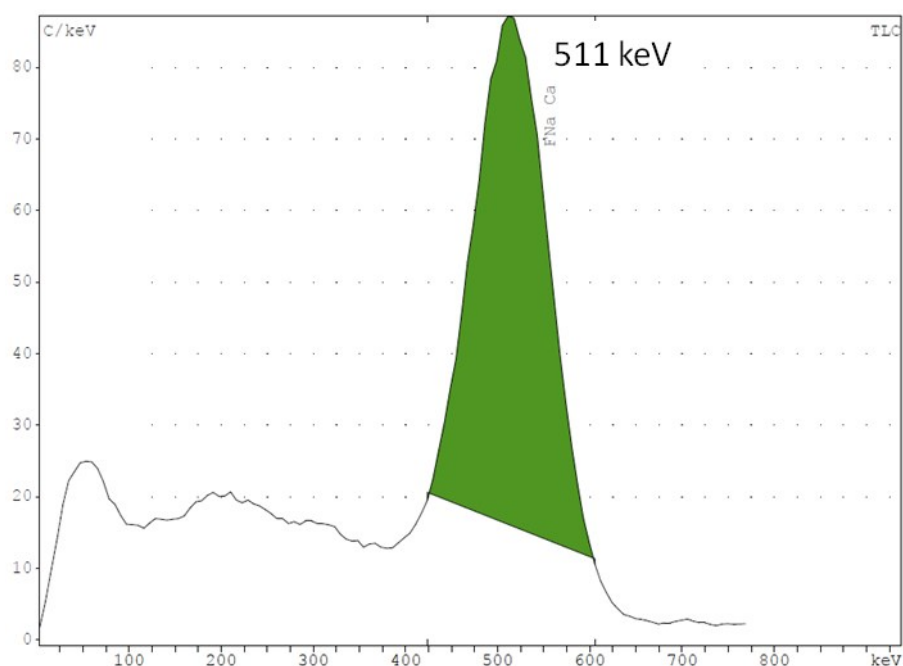
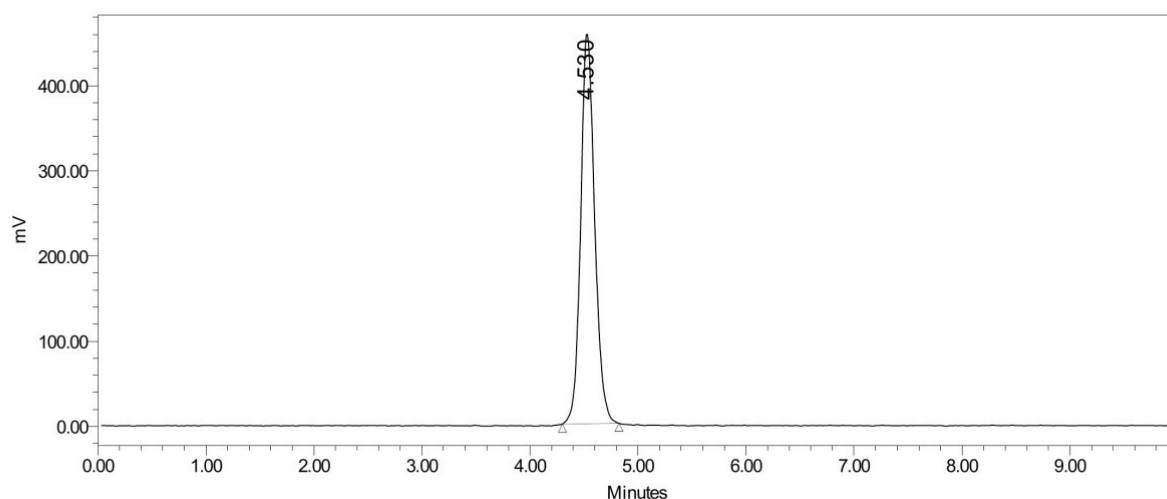


Figure S11. Gamma Ray spectrum of [¹⁸F]NaF



Channel: eSATIN-Ch1; Processed Channel: Channel 1; Result Id: 6833; Processing Method: NaF

Processed Channel Descr.: Channel 1

	Processed Channel Descr.	RT	Area	% Area	Height
1	Channel 1	4.530	4101106	100.00	457547

Figure S12. Representative analytical radio-HPLC profile of [¹⁸F]NaF synthesized on R1; $V_{inj.}$ =20 μ L, t_r =4.5 min, Dionex™ CarboPac™ PA10 (4×250 mm) from Thermo Scientific™ ; 0.1 M sodium hydroxide solution at 1 mL/min.